Available online at www.sciencedirect.com
SCIENCE DIRECT
Journal of Catalysis 233 (2005) 372–387
JOURNAL OF CATALYSIS
www.elsevier.com/locate/jcat

Kinetics, operando FTIR, and controlled atmosphere EXAFS study of the effect of sulfur on Pt-supported catalysts during CO oxidation

F.J. Gracia [a], S. Guerrero [a], E.E. Wolf [a,*], J.T. Miller [b], A.J. Kropf [c]

[a] *Department of Chemical Engineering, University of Notre Dame, Notre Dame, IN 46556, USA*
[b] *BP Research Center, E-1F, 150 W. Warrenville Rd., Naperville, IL 60563, USA*
[c] *Chemical Engineering Division, Argonne National Laboratory, 9700 S. Cass Avenue, Argonne, IL 60439, USA*

Received 22 December 2004; revised 18 March 2005; accepted 4 April 2005

Available online 13 June 2005

Abstract

The effect of the presence of sulfur on the state of the catalytic surface during oxidation reactions on supported Pt catalysts has been investigated by kinetic studies and operando infrared (IR) and in situ extended X-ray absorption fine structure (EXAFS) spectroscopies. The experimental results clearly show that the catalytic surface is not static, and the reaction atmosphere strongly affects the state of the surface and consequently the catalytic activity. The activity results show that the light-off temperature for CO oxidation increases with ex situ H_2S addition. In situ IR results show a shift of the linear CO band, indicating a change in the bonding of adsorbed CO due to the presence of sulfur. Continuous co-feeding of 20 ppm of SO_2 with the reactant mixture also increases the light-off temperature. Activity and IR results demonstrate that alumina acts as a sulfur storage reservoir. This delays the initial deactivation, but after extended time on stream in the presence of SO_2 the activities of the silica- and alumina-supported catalysts are similar. The results indicate that sulfur poisoning is not only due to blocking of the sites where oxygen preferentially adsorbs, but also to modification of the Pt–CO bonding.

Keywords: Sulfur poisoning; Pt/alumina; Pt/silica; Hydrocarbon oxidation; EXAFS; IR of adsorbed CO

1. Introduction

The presence of adsorbed species containing sulfur on metal surfaces can block reaction sites, induce changes in surface morphology due to faceting and preferentially segregate one component in multicomponent catalysts, enhance sintering, and alter the electronic structure of the metal. Many studies have contributed to the understanding of these processes and their effects on catalytic activity and selectivity during hydrocarbon conversion under reducing conditions, but less is known about the effects during oxidation reactions. Under reducing conditions the presence of sulfur in general decreases the activity; however, several papers have been published which report that during oxidation reactions, an increase in activity has been observed on Pt-supported catalysts.

The early literature on S poisoning comprises studies on the effect of pre-adsorbed sulfur that had been made at low pressures (below 10^{-6} Torr) by pulse techniques on single crystal samples. These results have been summarized in a review by Bartholomew [1] and in a monograph edited by Oudar and Wise [2]. Several mechanisms have been proposed in the literature [3] to describe the effect of sulfur compounds on supported Pt catalysts. These include: (1) rearrangement of Pt crystal structure, (2) electronic effects due to the presence of sulfur, (3) formation of surface Pt sulfate, and (4) formation of sulfate on the support or Pt/support interface. The results depend on the structure and composition of the metal surface (single crystal vs. dispersed), the reaction environment (ultrahigh vacuum (UHV) vs. atmospheric pressure and reducing vs. oxidizing atmospheres), the con-

* Corresponding author. Fax: +1 219 631 8366.
E-mail address: eduardo.e.wolf.1@nd.edu (E.E. Wolf).

0021-9517/$ – see front matter © 2005 Published by Elsevier Inc.
doi:10.1016/j.jcat.2005.04.016

centration and method of introduction of the sulfur (ex situ vs. in situ vs. operando), and the support used.

Restructuring of the Pt surface after interaction with sulfur compounds has been observed on single-crystal surfaces by transformation of Pt[100] into the Pt[111] face due to the lowering of the surface free energy [3], and due to faceting on Pt–Rh wires [4] and on supported Pt catalysts [5]. Oudar [6] reported that the adsorption of sulfur compounds on metal catalysts can cause modifications in both the structural and electronic properties of the metal, which change the metal's surface reactivity by weakening the electronic density of the surface as a result of sulfur's electronegative character. Using UHV-TPD, Gland et al. studied the adsorption of CO on polycrystalline Pt exposed to H_2S [7] and found that H_2S adsorption strongly decreases CO adsorption. These results suggested that the S effect is not only site blocking at short range, but that it also involves a long-range electronic effect, decreasing the bonding strength of CO on Pt. Yates et al. [8] also observed strong reduction in the CO adsorption capacity on a Pt(111) single crystal due to the adsorption of sulfur. The effect was attributed to a combination of the physical blocking of active Pt sites by sulfur and a perturbation of next-nearest-neighbor Pt sites, causing a decrease in the adsorption binding energy. Theoretical calculations by Ruckestein et al. [9] for model Pt clusters, consisting of either ten Pt atoms in the (111) orientation or nine Pt atoms in the (100) orientation, show that adsorbed S atoms decrease the electron density of the cluster, yielding more positively charged Pt atoms. Adsorbed S atoms inhibit the dissociative chemisorption of O_2 on Pt by inhibiting the electron transfer from Pt to the π^* antibonding molecular orbitals of O_2.

Bonzel and Ku [10] found that during CO oxidation at low pressures on Pt(100), adsorbed sulfur considerably weakens the CO–metal bond and that the rate of CO_2 formation on Pt(100) is completely inhibited at a sulfur coverage equal to or greater than 0.3. At this point, however, CO could still be adsorbed; this implied that the complete poisoning of the reaction should be due mainly to the inhibition of O_2 dissociation by sulfur instead of the blockage of CO adsorption. A similar result was obtained during S adsorption on Pt and Ni single crystals [6], and it was postulated that the effect of S on these metals is primarily electronic, reducing the availability of metal *d*-electrons and weakening the interaction with adsorbates. Feibelman and Hamann [11] studied the distance dependence of adsorbed sulfur on transition-metal properties and suggested that sulfur-induced changes in the reactant sticking probability, coverage, and activity on transition metal surfaces is, in fact, a result of perturbations in the electronic properties over distances exceeding nearest-neighbor metal sites. An IR study by Apesteguìa et al. [12] showed evidence of electronic effects due to pre-adsorbed sulfur on the adsorption of CO on a Pt/Al_2O_3 catalyst. The results showed a decrease in the CO adsorption band intensity and a positive 15 cm^{-1} shift in band frequency for CO adsorbed to sulfur-treated Pt when compared with CO adsorption on a clean Pt surface. From these experiments the authors concluded that sulfur altered the electronic properties of Pt, but these effects were localized.

Lambert et al. [13] showed that during C_3H_8 oxidation, adsorbed sulfur compounds on Pt(111) can promote its oxidation, which was attributed to the formation of a SO_x compound on an O_2 pre-covered Pt surface. Under UHV, the oxy-sulfided surface was active for the dissociative chemisorption of C_3H_8, which further enhanced its oxidation. No C_3H_8 dissociative adsorption was found on a clean Pt(111) surface or on a Pt(111) surface pre-adsorbed with SO_2 only. Spectroscopic studies [14] identified this surface as a chemisorbed sulfur complex bound to Pt in a bidentate geometry through two O atoms. Lambert et al. [13] found that CH_4 and C_2H_6 do not show activation similar to that of C_3H_8 because of the presence of stronger C–H bonds, and it is assumed that the initial H atom abstraction in C_3H_8 occurs on the secondary C atom. In a follow-up study, Lambert et al. [15] conducted propane oxidation experiments on a Pt(111) surface on which an AlO_x film had been deposited. The results showed an even greater enhancement of propane oxidation on AlO_x/Pt(111) after O_2 and SO_2 adsorption than that observed for a similarly treated Pt(111) surface. The increased activity is suggested to be a result of an AlO_x-induced stabilization of an adsorbed SO_4 complex, yielding a bifunctional catalyst. To determine the relevance of these experiments to practical highly dispersed catalyst systems, Lambert et al. [16] continued their studies on Pt/Al_2O_3. Sulfur poisoning was carried out by treatment of Pt/Al_2O_3 catalysts with a 1:1 mixture of SO_2 and O_2 at 1 bar and 673 K. Characterization results show that SO_2 poisoning resulted in Pt sintering and the formation of aluminum sulfate. Additional experiments showed that, at low metal loadings, Pt exists mainly as oxidized particles (PtO_2), which are not as active for C_3H_8 oxidation.

On supported Pt catalysts, sulfur compounds (H_2S, SO_2, and SO_3) can form sulfates on certain types of supports when the treatment is carried out in an oxidizing environment at sufficiently high temperatures ($\geqslant 400\,^{\circ}C$) and/or for a sufficiently long time on stream. It has been proposed that sulfate formation on the support occurs by the spillover of SO_3 to the support surface, followed by subsequent oxidation to SO_4^{-2}, most likely occurring at the Pt/support interface. The hydrocarbon oxidation activity of a $Pt–Rh/CeO_2–Al_2O_3$ three-way catalyst was investigated by Ansell et al. [17] for the reduction and oxidation of simulated exhaust-gas mixtures containing SO_2. For a reducing fuel-rich exhaust gas mixture, the presence of 20 ppm SO_2 in the feedstream caused severe deactivation for CH_4 and C_3H_8 oxidation reactions. A comparable fuel-lean oxidizing gas mixture showed enhanced oxidation activity for C_3H_8 and a negligible effect for CH_4 oxidation when 20 ppm SO_2 was included in the feedstream. Treatment of the $Pt–Rh/CeO_2–Al_2O_3$ catalyst in a reducing exhaust gas mixture including 20 ppm SO_2 at various temperatures caused the CO chemisorption capacity of the catalyst to be severely reduced [17]. The authors attributed some of this decrease

to thermally induced sintering, sulfate formation, and site blocking as a cause of adsorption inhibition. XPS studies of the fuel rich-aged catalyst confirmed the presence of a small amount of S, but a majority of the sulfur present was in the form of S^{6+} (SO_4^{-2}).

Meeyoo et al. [18] studied the activity of a 0.2% Pt/Al_2O_3 catalyst for the oxidation of CH_4. These authors found that the addition of either 20 ppm H_2S or 20 ppm SO_2 to the reactant gas stream (1.8% CH_4, 21% O_2, balance in He) resulted in a slight activity increase for CH_4 oxidation. However, this observation is contrary to many reports in the literature, including those of Golunksi et al. [17] and Wang [19], which show either a negligible effect or a slight deactivation of CH_4 oxidation due to sulfur poisoning of Pt/Al_2O_3 catalysts. Meeyoo et al. [18] suggest that the observed effects are a result of the increased catalyst acidity due to the formation of aluminum sulfate. However, changes in acidity do not entirely explain the sulfur-induced enhancement of hydrocarbon oxidation as shown by Burch et al. [20].

In summary, according to the current literature, under reduction conditions, S compounds interact with Pt active sites, altering the state of the Pt surface. This causes short-range site blocking and long-range electronic effects that alter surface-adsorbate interactions. Under oxidation reactions, however, the local structure of the metal-sulfur active site and how it changes with differing metals, supports, and reaction conditions is not well understood. Understanding these effects as a function of the type of metal, pretreatment, particle size, support, and reaction conditions can lead to the development of poison-resistant catalysts or catalysts with improved activity in the presence of S.

This paper presents a study of the effect of S compounds (H_2S and SO_2) on the activity of Pt supported on silica and alumina catalysts during CO oxidation. The activity measurements are complemented with in situ EXAFS and operando infrared (IR) spectroscopies to determine the state of the working surface under reaction conditions.

2. Experimental

2.1. Catalyst preparation

Pt catalysts supported on silica and alumina were prepared by incipient wetness impregnation of tetra-amine-platinum nitrate to avoid Cl poisoning [21,22]. Hydrogen chemisorption values were determined volumetrically by the double isotherm method at room temperature (RT) after pre-reduction at 250 °C on a Coulter Omnisorb 100 CX instrument. The following conditions were used in the preparation of the various catalysts studied.

2% Pt/silica. To 9.8 g of Davison 644 grade silica (290 m^2/g and 1.16 cc/g pore volume (PV)) was added 0.40 g of $Pt(NH_3)_4(NO_3)_2$ (PTA) in 15 ml H_2O made basic to a pH of 10.0 with concentrated NH_4OH. The catalyst was dried at 100 °C. Direct reduction of the dried catalyst gave a dispersion by hydrogen chemisorption at RT of 0.63.

To 36.0 g of Davison 644 grade silica was added 1.44 g of PTA in 56 ml H_2O at a pH of 5.5; this was dried at 100 °C. Calcination of the catalyst at 250 °C followed by reduction gave a dispersion of 0.33. Calcination of the catalyst at 600 °C followed by reduction gave a dispersion of 0.10.

2% Pt–5% CeO_2/silica. To 14.25 g of Davison 644 grade silica was added 1.89 g of $Ce(NO_3)_3{\cdot}6H_2O$ in 15.5 ml H_2O. The catalyst was dried overnight at 100 °C and calcined at 300 °C for 4 h. To 14.7 g of the Ce-silica support was added 0.60 g PTA in 15 ml H_2O; this was dried at 100 °C and reduced at 250 °C in flowing H_2 to give a dispersion of 0.72.

2% Pt/alumina. To 14.7 g Catapal alumina (SA = 190 m^2/g, PV = 0.45 cc/g) was added 0.60 g of PTA in 11 ml H_2O; this was calcined at 300 °C for 3 h. Reduction gave a dispersion of 0.68.

2% Pt–5% CeO_2/alumina. To 14.25 g of Catapal alumina was added 2.39 g of $(NH_4)_2Ce(NO_3)_6$ in 10 ml H_2O. The catalyst was dried overnight at 100 °C and calcined at 300 °C for 4 h. To 14.7 g of the Ce-alumina support was added 0.60 g PTA in 10 ml H_2O; this was dried at 100 °C and reduced at 250 °C in flowing H_2 to give a dispersion of 0.73. Table 1 summarizes the various catalysts prepared and their dispersions.

Table 1
Catalyst preparation and Pt dispersion of reduced catalysts

Sample	Catalyst	Dispersion (±0.02)
$Pt(0.10)/SiO_2$	2.0% Pt/SiO_2	0.10
$Pt(0.33)/SiO_2$	2.0% Pt/SiO_2	0.33
$Pt(0.63)/SiO_2$	2.0% Pt/SiO_2	0.63
$Pt(0.72)–CeO_2/SiO_2$	2.0% Pt–5% CeO_2/SiO_2	0.72
$Pt(0.68)/Al_2O_3$	2.0% Pt/Al_2O_3	0.68
$Pt(0.73)–CeO_2/Al_2O_3$	2.0% Pt–5% CeO_2/Al_2O_3	0.73

2.2. Catalytic activity

Catalytic activities were determined in two types of reactors. A ten-channel parallel microreactor was first used for high-throughput studies to obtain the main trends on the effect of H_2S pretreatment on Pt/SiO_2 catalysts. Then detailed kinetic information on the effect of SO_2 co-feeding was obtained with a tubular flow recycle reactor. Catalysts activities were obtained under diluted reactant concentrations: 1% CO in an oxidizing atmosphere with 5% or 10% O_2, balance in He. Unless specified otherwise, before reaction, the catalysts were reduced in hydrogen flowing at 100 cc/min at 150 °C.

The ten-channel microreactor [23] is made of stainless steel and has ten reaction wells (3/8-inch diameter, 2 inches long), each containing up to 200 mg of catalysts. The reactor is interfaced on line to a gas chromatograph (GC) through

a multiple-position valve, which selects the effluent from among the ten reaction channels for analysis. In some experiments not all ten wells were used, and in such a case, silica was used in the empty wells to maintain the same flow distribution in each well. A valve was used as a restrictor at the exit of the total stream to maintain a constant pressure drop throughout each well and to equalize their flow. The catalyst particles were prepared by pressing and crushing powders and sieving them between #18 and #30 Tyler meshes (1–0.6 mm size). The reactor system also has programmable electronic flow controllers to meter the various gases into the reactor; the total flow rate in each well was maintained at 60 cc/min (total flow of 600 cc/min). The reactor was placed in a furnace equipped with a temperature control to maintain its temperature constant and several thermocouples were used to measure the reactor temperature.

The recycle reactor consists of a quartz tube (12 inches long, 1/2-inch diameter) equipped with an external diaphragm pump to provide an external recycle loop. A thermocouple is placed in a thermocouple well in the center of the catalyst bed to monitor the temperature of the bed. The effluent flow rate was 130 cc/min, and the recycle ratio was about 20, to ensure operation at conditions equivalent to perfect mixing.

Gas chromatographic analysis of the effluent stream was carried out with a Hayesep Q column at room temperature in a GC (Varian 3300) equipped with a TC detector. The conversion data were reproducible within 5% accuracy. Reaction rates were calculated at various temperatures at less than 5% conversion to fulfill differential conversion operation in the ten-well reactor. In the recycle reactor, reaction rates were calculated in the whole conversion range because of the perfect mixing approximation obtained via the use of a large recycle ratio (> 20). Turnover frequencies were calculated from rate and the dispersion values obtained for the freshly reduced catalysts and plotted versus $1/T$ to obtain activation energies.

2.3. EXAFS data collection and analysis

Measurements made by extended X-ray absorption fine-structure (EXAFS) spectroscopy were made on the insertion-device beam line of the Materials Research Collaborative Access Team (MRCAT) at the Advanced Photon Source, Argonne National Laboratory. Measurements were made in transmission mode with ionization chambers optimized for the maximum current with linear response ($\sim 10^{10}$ photons detected/s). A cryogenically cooled double-crystal Si(111) monochromator with a resolution (ΔE) better than 2.5 eV at 11.564 keV (Pt L_3-edge) was used in conjunction with a Rh-coated mirror to minimize the presence of harmonics [24]. Spectra were acquired by continuously scanning the monochromator and stepping a multichannel scaler every 0.1 s (ca. 0.6 eV). Standard procedures based on WINXAS97 software [25] were used to extract the EXAFS data [26]. Phase shifts and backscattering amplitudes were obtained from EXAFS data for reference compounds: $Na_2Pt(OH)_6$ for Pt–O, H_2PtCl_6 for Pt–S, and Pt foil for Pt–Pt. $Pt(NH_3)_4(NO_3)_2$, H_2PtCl_6, and Pt foil were used for the Pt^{+2}, Pt^{+4}, and Pt^0 XANES references.

The sample was pressed into a cylindrical holder with a thickness chosen to give an absorbance ($\Delta\mu x$) of about 0.5 in the Pt edge region, corresponding to approximately 100 mg of catalyst. The sample holder was centered in a continuous-flow in situ EXAFS reactor tube (18 inches long, 0.75 inch diameter) fitted at both ends with polyimide windows and valves to isolate the reactor from the atmosphere. The catalysts were pretreated off line with flowing gases or reactants at temperatures similar to those used during pretreatment or reaction. After the prescribed treatment the sample was cooled to room temperature in the gas used for pretreatment or reaction, and then the cell with the gas used for pretreatment was isolated by closing of the valves fitted at both ends of the tube and moved to the EXAFS data acquisition room.

2.4. FTIR spectroscopy

Transmission infrared spectra of pressed disks (~ 14 mg) of Pt/SiO_2 were collected in situ and under operando conditions in an IR reactor cell placed in an FTIR spectrometer (Mattson; Galaxy 6020) at a resolution of 2 cm^{-1} and 30 scans/spectrum. The IR cell is equipped with NaCl windows, connections for inlet and outlet flows, and thermocouples connected to a temperature controller to monitor and control its temperature. The spectra were obtained in absorbance mode after subtraction of the background spectrum of the catalyst's disk under He atmosphere at the corresponding temperature. The samples were pretreated at various conditions before the study of CO adsorption and reaction. After pretreatment, the catalyst was cooled to room temperature in He, and 1% CO was added to the feed to measure CO adsorption. During CO oxidation experiments 10% O_2 was added to the 1% CO–He feed. In both experiments the heating rate was 1 °C/min, and the total flow was 120 cc/min.

3. Results

3.1. Poisoning by ex situ H_2S pretreatment

3.1.1. Activity measurements after ex situ H_2S poisoning

Initially, we studied the effect of poisoning by treating the pre-reduced catalysts ex situ in a quartz reactor with diluted H_2S (0.3% H_2S in H_2) at either 25 or 200 °C for 2 h. The reduced catalysts were exposed to air at RT and thus were partially oxidized before the addition of H_2S. Then, 100 mg of the treated catalysts was loaded into the ten-channel reactor and reduced in situ at 200 °C for 2 h in 40 cc/min of a mixture of 50% H_2 in He. The reaction was carried out in a mixture of 1% CO–5% O_2 in He.

In the absence of S, the light-off temperature (LOT, temperature at 50% conversion) for Pt/silica increases with increasing dispersion [22]. The LOT is about 25 °C higher for Pt(0.10)/silica compared with Pt(0.33) and Pt(0.63)/silica. Poisoning of the Pt/silica catalysts by H_2S increased the LOT compared with the unsulfided catalysts of the same dispersion. There was no significant difference on the final activity of the catalyst when H_2S was added at either 25 or 200 °C. As the dispersion of Pt increases, the LOT increases. For example, the LOT increased by almost 50 °C for ($Pt(0.63)/SiO_2$), whereas the increase in the LOT was only 22 °C for ($Pt(0.10)/SiO_2$). Although the S-free activity of the smaller particles is higher, there is a greater loss in activity due to S poisoning. As a result, the activities of all of the S-poisoned catalysts are nearly the same, despite the differences in particle size.

Conversion vs. temperature results obtained in a recycle reactor, unlike those observed in the ten-channel parallel reactor, showed little difference between the H_2S-treated catalysts and the unpoisoned samples. These results are explained later based on the IR studies and other results described below.

3.1.2. EXAFS characterization after ex situ H_2S poisoning

The Pt/silica catalysts with different dispersions were pre-reduced and exposed to air at room temperature before saturation with flowing H_2S. In previous work, we found that the extent of Pt oxidation is particle size-dependent and increases with increasing dispersion [22]. EXAFS analysis of these catalysts [not shown] indicate the presence of Pt–Pt, Pt–S, and Pt–O bonds, except for Pt/silica with 0.1 dispersion, which showed only Pt–Pt bonds. EXAFS data were also obtained after reduction of the H_2S poisoned catalysts under conditions similar to those used before the catalytic reaction (250 °C in a mixture of 5% H_2 in He for 1 h, and cooled to room temperature in the flowing H_2 mixture). Table 3 summarizes the XANES and EXAFS results for the reduced H_2S-poisoned Pt/silica samples with different dispersions.

Fig. 1 shows the k^2-weighted Fourier transform of the raw EXAFS data ($k = 2.75$–13.1 Å^{-1}) for the Pt/silica catalysts. The Fourier transforms of these results show several peaks for Pt–Pt (between about 1.8 and 3.1 Å), which overlap with the Pt–S peak at about 2.9 Å. The peak positions in the Fourier transform do not represent the scattering distances, since the raw EXAFS data have not been phase corrected. The coordination number (CN) and bond distance of 11.6 and 2.77 Å, respectively, for the S-poisoned ($Pt(0.10)/SiO_2$) confirm that this catalyst possesses large Pt crystallites; for example, the CN of Pt foil is 12 with a bond distance of 2.77 Å. Higher Pt–Pt coordination shells, consistent for large particles, are present at 3.6, 4.5, and 5.3 Å. These particles are sufficiently large that the signal is dominated by the bulk structure. Therefore it was not possible to detect oxidized Pt–O bonds by XANES or Pt–S bonds by EXAFS at the particle surface (Fig. 1a). As the Pt dispersion increases, there is a small increase in the white line intensity and the number of Pt–S bonds (Table 3). In addition, as the dispersion increases, the relative size of the Pt–S signal also increases (see, for example, Fig. 1b for $Pt(0.63)/SiO_2$). The XANES and EXAFS are consistent with oxidation of the surface Pt atoms to Pt^{2+} due to Pt–S bonds. The core of the particle, however, remains metallic. It should also be noted that these XAFS results were *not* obtained under operando conditions,

Table 2
Effect of ex-situ H_2S poisoning in the co conversion of Pt/SiO_2 catalysts

Sample	Treatment	T_{50} (°C)	ΔT_{50} (°C)
$Pt(0.10)/SiO_2$	No S	135	22
	H_2S poisoned	157	
$Pt(0.33)/SiO_2$	No S	111	45
	H_2S poisoned	156	
$Pt(0.63)/SiO_2$	No S	112	49
	H_2S poisoned	161	

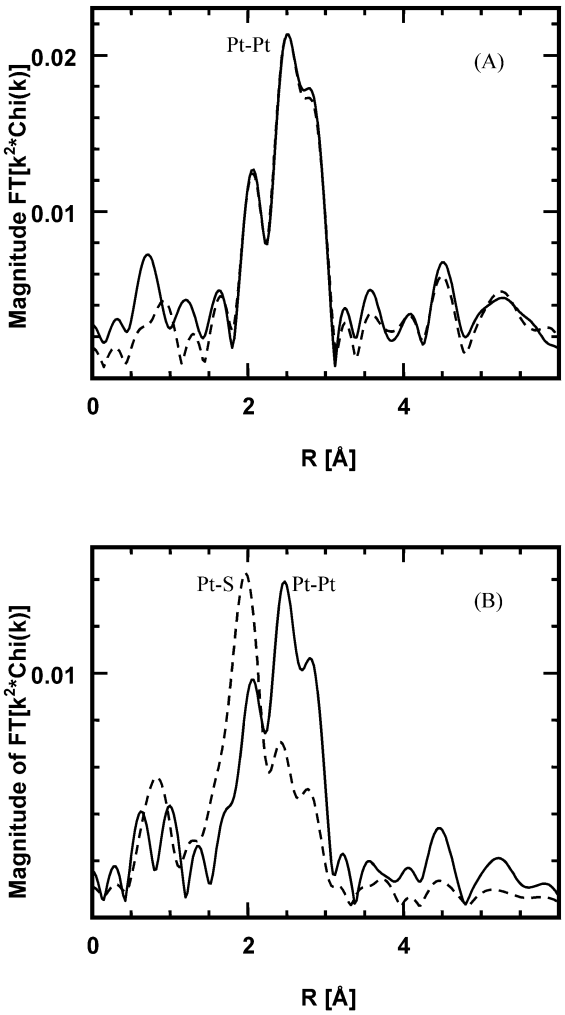

Fig. 1. Magnitude of the k^2-weighted FT ($k = 2.75$–13.3 Å^{-1} for (A) $Pt(0.10)/SiO_2$): solid line, reduced in H_2 at 250 °C; dashed line, pre-reduced at 250 °C; air oxidized at RT, H_2S at RT, and reduced at 250 °C. (B) $Pt(0.63)/SiO_2$, same treatments as in (A).

Table 3
EXAFS and XANES fits: 2% Pt/SiO_2 catalysts with different dispersion after reduction and H_2S/reduction

Sample	Fraction Pt^{+2}	Fraction Pt^0	Scattering atoms	CN (±10%)	R (Å) (±0.02)	Δ DWF ($\times 10^3$ Å^2)	E_0 (eV)
Pt(0.10)/SiO_2	–	1.0	Pt–Pt	12.0	2.77	1.6	−1.8
Pt(0.10)/SiO_2 + H_2S	–	1.0	Pt–Pt	11.6	2.76	1.6	−1.5
Pt(0.33)/SiO_2	–	1.0	Pt–Pt	9.3	2.75	1.6	−3.1
Pt(0.33)/SiO_2 + H_2S	0.05	0.95	Pt–Pt	7.2	2.75	1.6	−2.7
			Pt–S	1.0	2.33	4.0	3.2
Pt(0.63)/SiO_2	–	1.0	Pt–Pt	7.8	2.74	1.6	−3.6
Pt(0.63)/SiO_2 + H_2S	0.80	0.20	Pt–Pt	3.4	2.73	1.6	−3.5
			Pt–S	2.0	2.33	4.0	3.1

and thus they represent only the *initial* state of the surface before oxidation reactions.

3.1.3. Operando IR experiments after ex situ H_2S poisoning

In situ IR results under reaction conditions, i.e., under operando conditions (1% CO–5% O_2) of the S-free and ex situ H_2S-poisoned Pt(0.63)/SiO_2 catalyst, starting at about 100 °C, are shown in Fig. 2. For the S-free catalysts, at 100 °C the frequency of absorption (2071 cm^{-1}) is consistent with CO linearly adsorbed on metallic Pt (L-CO). As the temperature and oxidation rate increase, the CO surface coverage remains nearly constant up to about 166 °C. Above 166 °C, the reaction ignites and the CO coverage decreases below the detection limit of the spectrometer, which is characteristic for a Langmuir–Hinshelwood (L-H) mechanism of CO oxidation and which has been observed previously [22]. For the S-poisoned catalyst, the CO absorbance is similar to that of the S-free catalyst, which was not expected, because of the presence of S. The frequency of the adsorbed CO band, however, is significantly higher (2086 cm^{-1}) than that on metallic Pt, indicating that CO is more weakly bonded to Pt in the S-poisoned catalyst. On the S-poisoned catalyst, ignition occurs at about 198 °C, as indicated by the abrupt change in the CO surface coverage, which decreases below the detection limit 32 °C higher than observed for the S-free catalyst and is consistent with the increase in LOT observed in the parallel reactor. The results indicated that although there is a significant decrease in activity, the L-CO coverage is similar to that of the unpoisoned catalysts, indicating that CO adsorption is *not* the cause of the activity decrease.

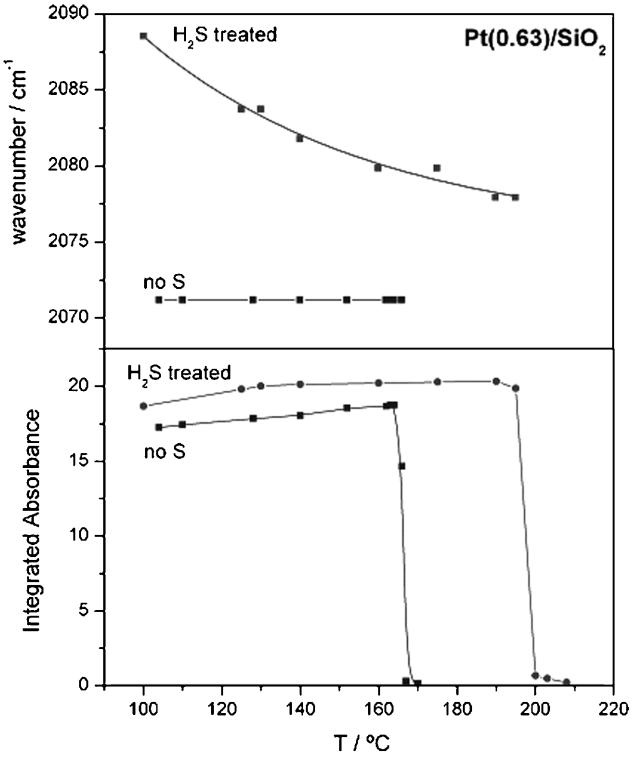

Fig. 2. Frequency shift and integrated absorbance versus temperature of L-CO band on 2% Pt(0.63)/SiO_2 after H_2S treatment. Reaction conditions: 1% CO, 5% O_2 in He. Temperature ramp 1 °C/min. Upper panel, wavenumber; lower panel, integrated absorbance (IA).

3.2. Poisoning during SO_2 co-feeding

3.2.1. Activity measurements during SO_2 co-feeding

During oxidation reactions, it is likely that S will be present as SO_2. For gasoline with 300 ppm of sulfur, the exhaust gases entering the TWC would contain about 20 ppm of SO_2 [27]. Thus, to emulate the S concentration in the exhaust gas from the engine, 20 ppm of SO_2 was added to the reactant mixture of 1% CO–10% O_2 in He and continuously fed to the catalyst.

Activity results are presented in Figs. 3 and 4 for Pt/silica and Pt/alumina catalysts. The circles correspond to the conversion data recorded in the absence of SO_2 and the squares to the data recorded in the presence of SO_2. Fig. 3A shows results for catalysts supported on alumina and silica with similar Pt dispersion, and Fig. 3B shows results for a Pt-ceria supported on alumina catalyst.

The LOT of Pt catalysts supported on alumina does not change significantly in the presence of SO_2 compared with Pt supported on silica, as shown in Fig. 3. This at first suggests an improved resistance to S poisoning by the alumina support. In the absence of SO_2, Pt supported on silica and alumina shows about the same activity for CO oxidation (filled and empty circles). But upon the addition of 20 ppm of SO_2 in the gas feed, the ignition temperature increases by only 5 °C during the *first run* in the alumina-supported sample compared with 31 °C in the case of the silica-supported catalyst. Since the two samples have similar metal disper-

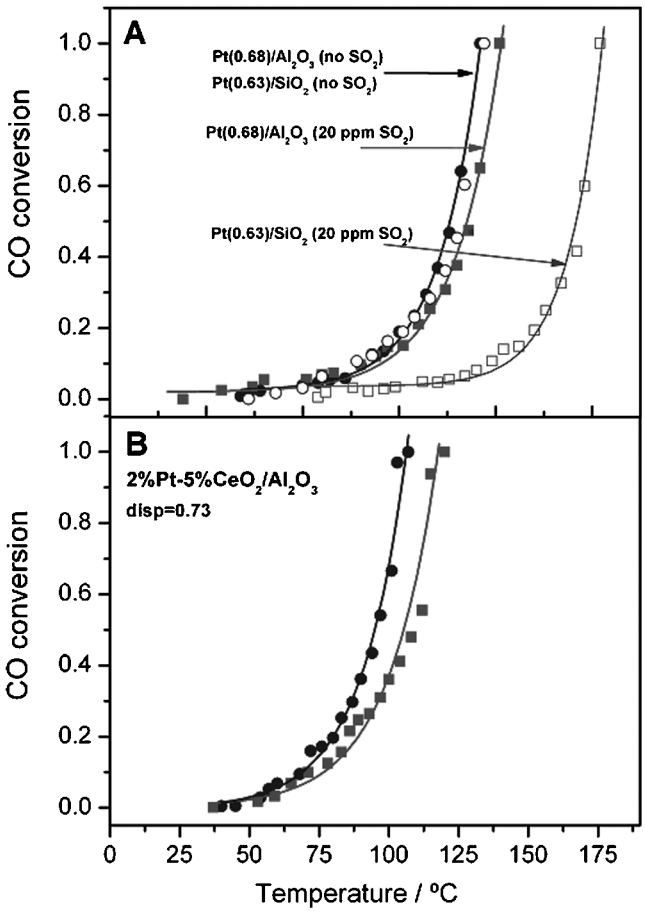

Fig. 3. Effect of SO_2 in the activity of Pt/SiO_2, Pt/Al_2O_3 and $Pt–CeO_2/Al_2O_3$ catalysts during CO oxidation. Reaction conditions: 1% CO–10% O_2 in He. Recycle reactor. Temp. ramp, 1 °C/min. ○, ●, No SO_2. ■, First run with SO_2. □, Second run with SO_2.

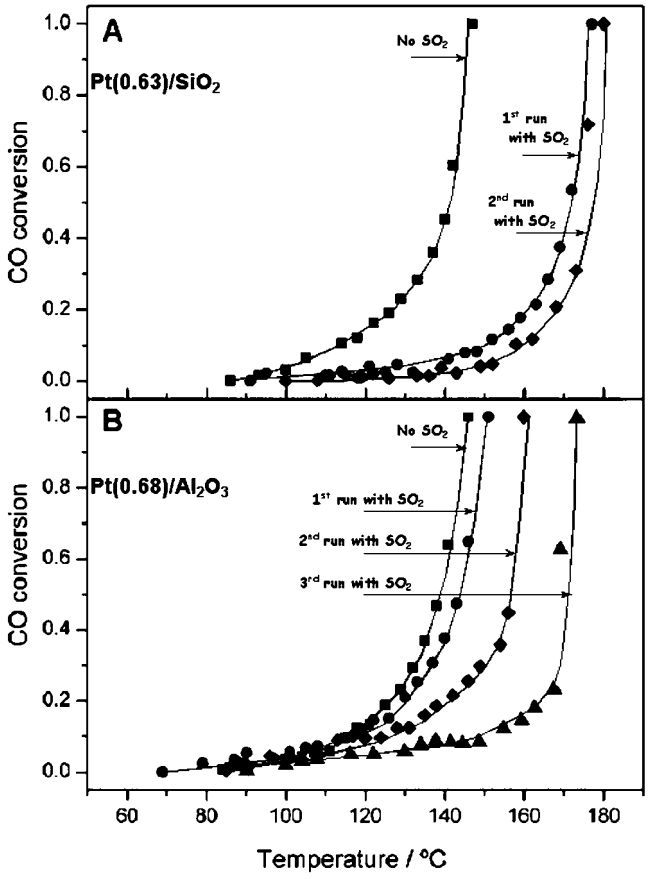

Fig. 4. Conversion versus temperature of Pt supported on SiO_2 and Al_2O_3 catalysts during CO oxidation in the presence of SO_2 after repeated runs. Reaction conditions: 1% CO–10% O_2 in He. Recycle reactor. Temperature ramp, 1 °C/min. ■, Reaction with no SO_2. ●, First reaction with 20 ppm of SO_2. ◆, Second reaction with 20 ppm of SO_2. ▲, Third reaction with 20 ppm of SO_2.

sions (0.68 and 0.63, respectively), this difference can be explained only by the presence of the support. In the literature it has been proposed that the presence of SO_2 leads to the formation of sulfates on the alumina surface, which thus becomes a sulfur trap. This would allow the Pt surface to appear not to be affected as strongly as in the case of the silica support in this short time on stream (TOS) run. Fig. 3B also shows that the increase in LOT is relatively small for the ceria-promoted alumina catalyst, probably for the same reason as for alumina. The addition of cerium oxide to Pt/silica (not shown in Fig. 3) significantly decreases the LOT (26 °C compared with $Pt(0.63)/SiO_2$). In the presence of S, however, the activity is the same as that of the Pt without Ce, indicating poisoning of the apparent promotional effect of Ce.

The evolution of the activity with TOS of the poisoned catalysts was studied on $Pt(0.63)/SiO_2$ and $Pt(0.68)/Al_2O_3$, and the CO conversion was measured after consecutive reactions in the presence of SO_2 (Fig. 4). After the first reaction the sample was cooled to room temperature in He and treated in 150 cc/min of H_2 at 300 °C for 2 h. Then the sample was again cooled to room temperature in He and the reaction mixture was started. The same procedure was repeated for the third and fourth runs. In every case the reactor temperature was increased until 100% CO conversion was obtained.

The CO conversion data for successive reactions on $Pt(0.63)/SiO_2$ (Fig. 4A) show that the difference between the first and second runs is small on the silica-supported catalyst. A third run did not show major differences compared with the second one. This indicates that when silica is the support, poisoning of the Pt surface occurs almost completely during the first run.

In the case of the alumina-supported catalyst (Fig. 4B), sulfur poisoning between runs is more gradual, with a small effect between the first and second runs and considerable change after the third run. There is only a 5 °C increase in the LOT between the first and second runs, but the LOT increases by 18 and 33 °C for the second and third runs, respectively. It is noteworthy that the activities of both silica- and alumina-supported catalysts are similar after four consecutive runs. This indicates that when the extent of the poisoning has reached its pseudo-equilibrium coverage, the activity becomes independent of the support. These results show that the support acts as a storage reservoir that might

Table 4
Activity results (recycle reactor) of the effect of SO_2 during co oxidation

T (°C)	Pt/SiO_2						Pt/CeO_2–SiO_2		Pt/Al_2O_3		Pt/CeO_2–Al_2O_3	
	H/Pt = 0.10		H/Pt = 0.33		H/Pt = 0.63		H/Pt = 0.72		H/Pt = 0.68		H/Pt = 0.73	
	No SO_2	20 ppm SO_2	No SO_2	20 ppm SO_2	No SO_2	20 ppm SO_2	No SO_2	20 ppm SO_2	No SO_2	20 ppm SO_2	No SO_2	20 ppm SO_2
						TOF (s^{-1})						
110	0	0	0.08	0.02	0.03	0.01	0.09	0	0.03	0.03	**0.27**	0.15
125	0	0	0.15	0.04	0.06	0.01	**0.27**	0	0.06	0.04	**0.27**	**0.27**
150	0.08	0	**0.57**	0.16	**0.29**	0.03	**0.27**	0.02	**0.28**	0.18	**0.27**	**0.27**
175	0.29	0.09	**0.57**	**0.54**	**0.29**	**0.27**	**0.27**	0.19	**0.28**	**0.28**	**0.27**	**0.27**
						LOT (°C)						
	192	213	135	160	141	172	115	173	139	144	96	110

initially delay the effect of S reaching the Pt surface. This effect disappears when saturation coverage of the support is reached after sufficient exposure of the alumina surface to sulfur. Again, it is clear that the state of the surface is determined by the reaction. Sufficient TOS must be allowed to reach the saturation state; otherwise incorrect conclusions can be drawn about the effect of the support on the activity of supported catalysts.

The turnover frequencies (TOFs) at various temperatures are summarized in Table 4. The dispersions determined by hydrogen chemisorption for the S-free catalysts were used to calculate the TOF, and the number of Pt atoms exposed in the poisoned catalysts was assumed to be identical to that in the S-free catalyst. The values printed in boldface indicate reaction rates at 100% CO conversion in the recycle reactor. For the silica-supported catalysts, the difference in the LOT between the fresh and poisoned samples (ΔT_{50}) appears to depend on the average particle size (expressed as metal dispersion), but to a smaller extent compared with the H_2S-poisoned catalysts. For the catalyst with lowest dispersion, $\Delta T_{50} = 21\,^{\circ}C$, whereas for the catalysts with dispersion of 0.33, $\Delta T_{50} = 25\,^{\circ}C$, and for the catalyst with highest dispersion (H/Pt = 0.63), $\Delta T_{50} = 31\,^{\circ}C$.

From the above results it is clear that the *continuous* presence of 20 ppm of SO_2 in the feed increases the LOT of Pt-supported catalysts in the recycle reactor, which is observed only during the ex situ H_2S poisoning experiments in the parallel reactor. This appears to be a contradictory result at first, but as explained later, is consistent with the characteristics of each reactor.

3.2.2. *In situ and operando IR experiments during SO_2 co-feeding*

To further investigate the poisoning effect of SO_2 during CO oxidation, the reaction was carried out in situ under reaction conditions, that is, under operando conditions in the IR reactor. An experiment under CO only would be in situ but not operando. After the standard pretreatment of the wafer in 120 cc/min of H_2 at 200 °C for 3 h and then cooling to 100 °C, the reactant mixture containing 1% CO, 10% O_2, and 20 ppm SO_2 in He was fed into the reactor. The spectra were collected at various temperatures, with the use of a temperature ramp of 1 °C/min. Fig. 5 shows the results of the CO oxidation with and without SO_2 on the Pt/SiO_2 catalyst with the highest dispersion ($Pt(0.63)/SiO_2$). The upper panel displays the wavenumber change of the linearly adsorbed CO band as a function of temperature. The shift in the wavenumber of the L-CO band for the poisoned catalyst during the first run is only 3 cm^{-1} and remains constant with

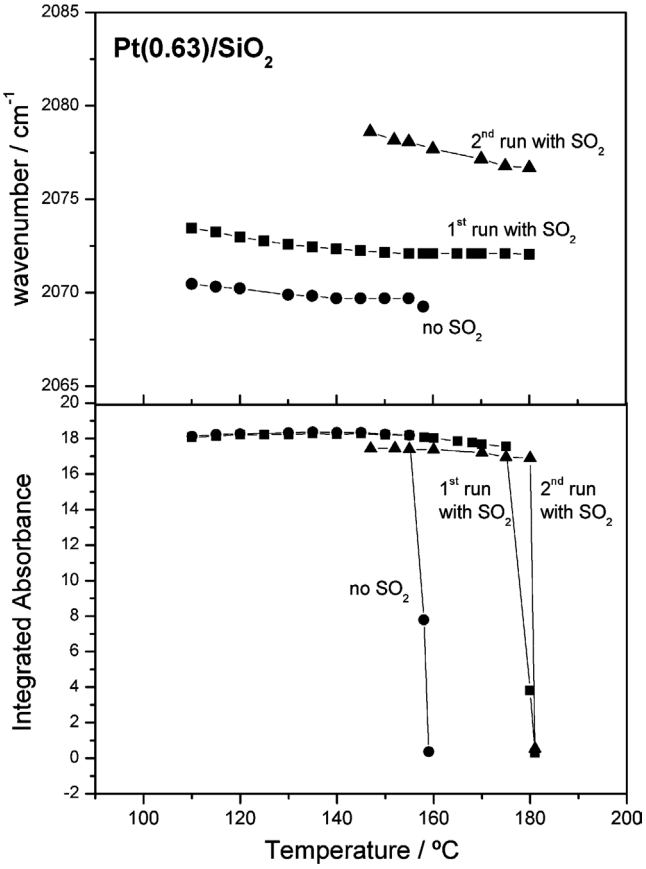

Fig. 5. Frequency shift and integrated absorbance versus temperature of the L-CO band adsorbed on 2% $Pt(0.63)/SiO_2$ during CO oxidation in the presence of SO_2 after repeated runs. Reaction conditions: 1% CO, 10% O_2 in He. Temperature ramp, 1 °C/min. Upper panel, wavenumber; lower panel, integrated absorbance (IA).

temperature until the catalyst reaches ignition. The lower panel displays the corresponding integrated absorbance (IA) of the adsorbed CO band versus temperature. The L-CO band also shows that in the presence of SO_2 the ignition temperature increases, as indicated by the sharp decrease in CO absorbance, consistent with the activity results obtained with the recycle reactor. As in the case of H_2S poisoning (Fig. 2), and contrary to expectations, before ignition the IA of the L-CO band is similar to that during reaction *without* SO_2, and yet the ignition temperature has increased by 22 °C.

Additional exposure to SO_2 in a second run led to an additional increase in the frequency of absorption of about 5 cm^{-1}, but the ignition temperature was similar. The absorption frequency of L-CO on the SO_2 poisoned Pt/SiO_2 catalyst was also similar to that for the H_2S poisoned catalyst after oxidation at high temperature (see Fig. 2). In agreement with the activity results, the IR spectra show that SO_2 poisoning of Pt supported on silica is evident after the first run, showing no storage effect by the silica support.

The results of a similar IR spectra obtained on the $Pt(0.68)/Al_2O_3$ sample are presented in Fig. 6. As in the silica-supported catalyst, the integrated CO absorbance before ignition during the first run with 20 ppm of SO_2 was the same as the absorbance found in the absence of SO_2. Unlike on Pt-supported on silica, however, there was no shift in the wavenumber of the CO band, and the ignition temperature was the same *with or without* SO_2 in the feed (only one data set shown). This indicates little effect of SO_2 on the alumina-supported Pt in the first run, which is consistent with the activity results in Fig. 3.

The flow pattern in the IR-cell reactor is a boundary-layer-type flow; hence, it is expected that the capture of SO_2 in the alumina support is less in the IR reactor. Consequently, the poisoning effect during the first run with SO_2 is almost imperceptible. When the reaction is carried out a second time with SO_2 there is a shift of 5 to 10 cm^{-1} in the wavenumber of the CO and a 16 °C increase in the ignition temperature. During the third run with SO_2, the shift in the wavenumber has increased by 15 cm^{-1} and the LOT is 35 °C higher. Finally, after four consecutive runs with SO_2, ignition occurred at 210 °C and the wavenumber of the L-CO band shifted by 25 cm^{-1} compared with that on the reduced, S-free catalyst. After the fourth run, the frequency of L-CO was similar to that of Pt/silica poisoned by SO_2 (see Fig. 5) and did not change with temperature. It should be noted that during these runs, the catalyst was reduced before each reaction, and that the reactions were restarted at 100 °C, which, as shown later, already altered the sulfur coverage and integrated CO absorbance, compared with runs started at RT.

The IR results for $Pt(0.68)/Al_2O_3$ showing an increase in ignition temperature with increasing SO_2 exposure agree very well with the increase in LOT with increasing SO_2 poisoning observed in the recycle reactor (Fig. 4). Fig. 7 shows the entire IR spectra of the $Pt(0.68)/Al_2O_3$ during CO oxidation without SO_2 and the consecutive runs with a co-feed of 20 ppm of SO_2. These spectra correspond to the experiments described in Fig. 6. Each IR spectrum was obtained under reaction conditions at 100 °C. With every consecutive run with SO_2 (except for the first one) there is an increase in the absorbance of the bands at 1045 cm^{-1}, 1170 cm^{-1}, 1290 cm^{-1}, and 1360 cm^{-1}. These bands have been identified in the literature as aluminum sulfates [28], with their suggested structure is depicted in Fig. 7.

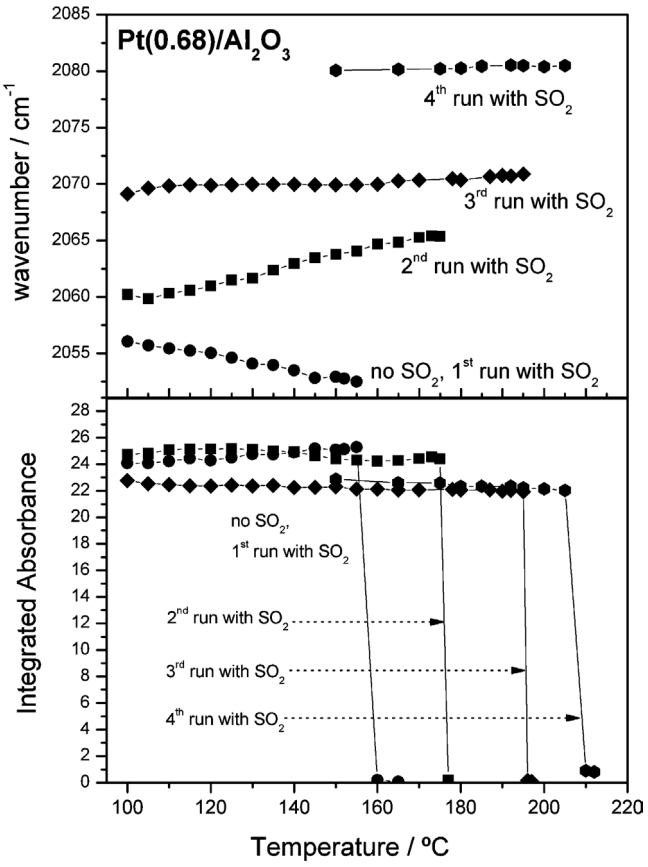

Fig. 6. Frequency shift and integrated intensity versus temperature of the L-CO band adsorbed on 2% $Pt(0.68)/Al_2O_3$ during CO oxidation in the presence of SO_2 after repeated runs. Reaction conditions: 1% CO, 10% O_2, 20 ppm SO_2 in He. Temperature ramp, 1 °C/min. Upper panel, wavenumber; lower panel, integrated absorbance (IA).

3.2.3. *Accelerated poisoning*

Because during the consecutive runs the catalyst was reduced before each run, thus refreshing the surface after the previous reaction, a new sample of $Pt(0.68)/Al_2O_3$ was poisoned overnight with 20 ppm of SO_2 in He at 200 °C (without CO or O_2) to ascertain the effect of long-term SO_2 exposure. After poisoning, the catalyst was cooled to room temperature and the reaction mixture was introduced into the reactor. In contrast with the IR results in Figs. 2, 5, and 6, the IR spectra in this case were obtained *without* prior reduction and before reaction. The IA of the L-CO band, collected at RT and at increasing temperatures, is shown in Fig. 8. It can be seen that the IA of the L-CO band is about 5 units at room temperature, which is low compared with the value of about 25 units for the S-free catalyst (Figs. 5 and 6). As the tem-

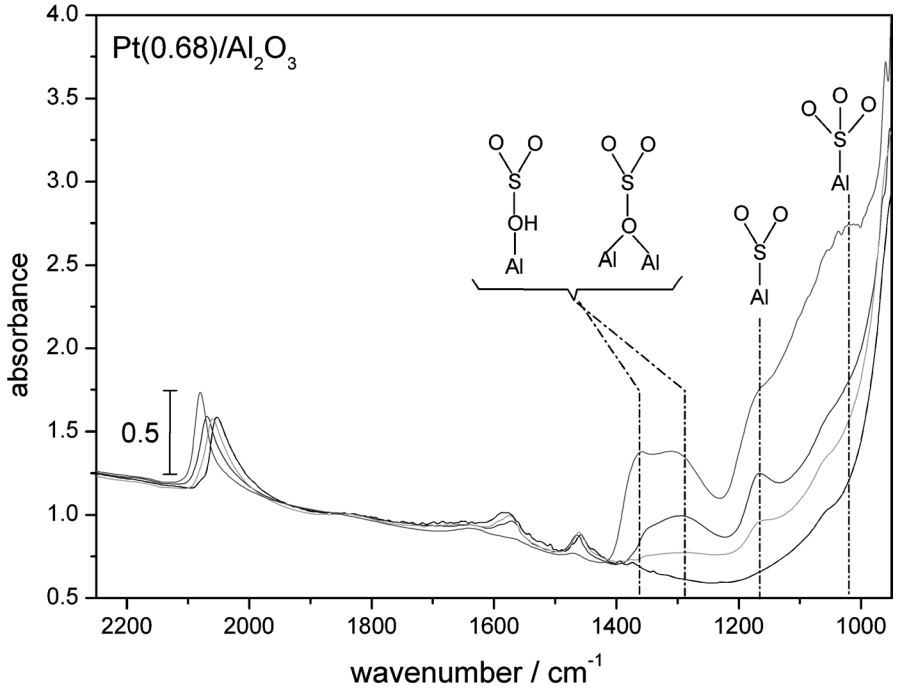

Fig. 7. IR spectra during successive reactions of CO oxidation on a 2%Pt(0.68)/Al_2O_3 catalyst. Reaction conditions: 1% CO, 10% O_2, 20 ppm SO_2 in He. Temperature ramp, 1 °C/min. Black line, run without SO_2 and first run with 20 ppm SO_2. Green line, second run with 20 ppm SO_2. Blue line, third run with 20 ppm SO_2. Red line, fourth run with 20 ppm SO_2.

perature increases, however, the integrated absorbance also increases by a factor of about 3, demonstrating that the *reaction gases* are modifying the catalyst surface. Two important results are observed here: first the long-term treatment in SO_2 in the *absence* of the reaction significantly poisoned the Pt surface, leading to a relatively low value of the L-CO absorbance at RT. Equally significant is the fact that, during *heating* in the reaction mixture to reach the reaction temperature, the reactants removed some of the adsorbed S as the L-CO absorbance increased with temperature. The results in Fig. 8 also show that pre-reduction by H_2, before SO_2 poisoning, has little effect on the L-CO band.

When the accelerated poisoning experiment (SO_2/He, 12 h, 200 °C) was conducted without cooling of the catalysts to room temperature, but instead by introduction of the reaction mixture at 200 °C, there was no CO adsorption immediately after feeding of the reactants (1% CO–10% O_2 in He without SO_2). After 1 h under reaction conditions at 200 °C, however, the CO absorbance reached a level similar to that observed before the poisoning treatment (not shown). Upon the introduction of feed containing SO_2, the catalysts responded in a way similar to that observed after the fourth run shown in Fig. 7; that is, there is no apparent support effect because it was saturated with SO_2 and the LOT was at its highest value. This clearly shows that the state of the catalytic surface depends on the initial conditions, composition of the reactants, SO_2 concentrations, temperature, and TOS.

3.2.4. *EXAFS Characterization of SO_2 poisoned catalysts*

The Pt/silica with different dispersions and Pt/alumina catalysts were pre-reduced and tested for catalytic oxidation of CO with 20 ppm SO_2. The XANES and EXAFS analysis (in air) (Table 5), following the reaction shows significant amounts of oxidized Pt (Fig. 9a) and the presence of Pt–Pt and Pt–O bonds, with no Pt–S bonds (Fig. 9b). From the Fourier transform of the EXAFS, all samples have metallic Pt; thus this must be included in the XANES fit. For several samples, the height of the white line was larger than the Pt^{2+} reference, and no fit could be obtained with only Pt^{2+} and Pt^0. However, excellent fits were obtained with a linear combination of Pt^{4+} and Pt^0. Acceptable fits were also possible using Pt^{2+}, Pt^{4+}, and Pt^0, which resulted in about 25% less metallic Pt. Although the absolute values of the various Pt oxidation states differ with the two fits, the trends are the same.

The XANES, therefore, should be used to identify trends in the catalysts' oxidation state, rather than quantitative values of the fraction of each catalyst present on the surface. For Pt/silica with different dispersions, the XANES show that the extent of Pt oxidation increases with decreasing particle size. For example, for the largest particles about 10% of the Pt is oxidized, whereas for the smallest particles about 35% is oxidized. The degree of oxidation of the Pt/alumina catalysts is very similar to, or perhaps slightly higher than, that observed on silica. For catalysts with dispersions around 0.7, the Pt–Pt coordination numbers (CN) are small, less than about 3. The true CN would be higher, since not all of the Pt is metallic. In Pt(0.63) the fraction of metallic Pt is 0.65 (fraction obtained by fitting with Pt^{4+} and Pt^0); thus the true Pt–Pt CN would be 4.5. The fraction of metallic Pt decreases to 0.5 if the XANES fits also include Pt^{2+}, and the true CN is 5.8. For either estimate, the particles are small, less than

Table 5
EXAFS results for 2% catalysts poisoned by SO_2 during oxidation reaction

Composition	Dispersion (%)	Fraction Pt^{4+}	Fraction Pt^0	Scattering atoms	CN	R (Å) (±0.02)	Δ DWF ($\times 10^3$ Å^2)	E_0 (eV)
SiO_2	0.10	0.10	0.90	Pt–Pt	10.0	2.77	1.0	−1.6
				Pt–O	0.5	2.05	1.5	1.6
SiO_2	0.33	0.25	0.75	Pt–Pt	5.1	2.74	1.6	−3.7
				Pt–O	2.1	2.05	1.5	0.5
SiO_2	0.63	0.35	0.65	Pt–Pt	2.9	2.71	1.6	−5.4
				Pt–O	2.7	2.05	1.5	−0.2
5%CeO_2–SiO_2	0.72	0.35	0.65	Pt–Pt	2.7	2.71	1.6	−5.6
				Pt–O	3.0	2.05	1.5	0.2
Al_2O_3	0.68	0.45	0.55	Pt–Pt	1.6	2.65	1.6	−6.0
				Pt–O	3.4	2.04	1.5	−0.5
Al_2O_3 (4X SO_2)	0.68	0.25	0.75	Pt–Pt	2.3	2.71	1.6	−2.8
				Pt–O	2.7	2.05	1.5	0.6
5%CeO_2–Al_2O_3	0.73	0.30	0.70	Pt–Pt	3.1	2.71	1.6	−5.3
				Pt–O	2.5	2.05	1.5	0.2

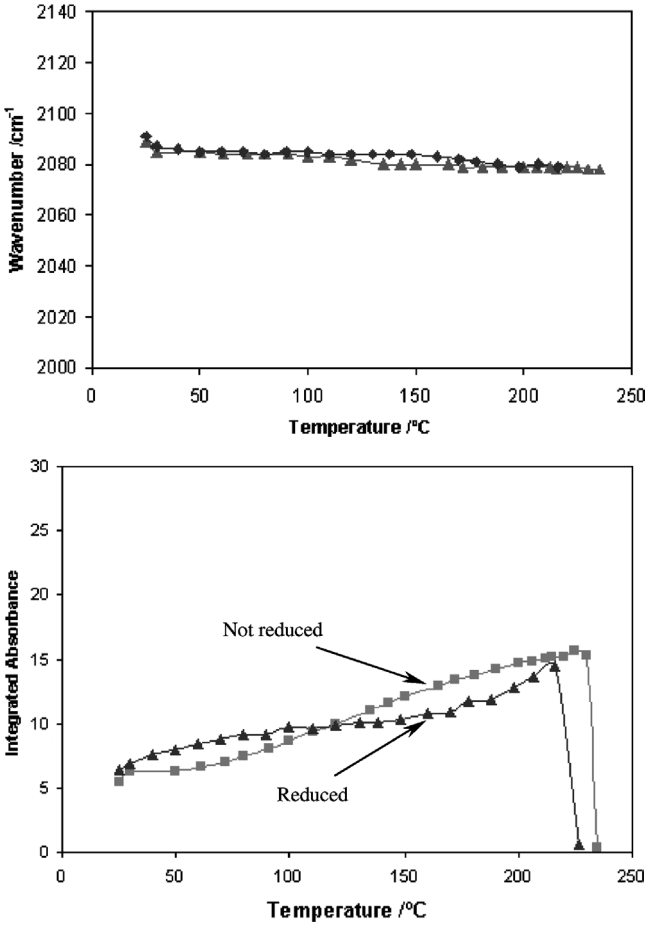

Fig. 8. Frequency shift and integrated intensity versus temperature of the L-CO band adsorbed on 2%Pt(0.68)/Al_2O_3 after overnight exposure to 20 ppm of SO_2 in He at 200 °C, followed by cooling to RT and exposure to reaction gases.

10 Å [29]. Consistent with this small particle size, the Pt–Pt bond distance is about 2.72 Å.

The EXAFS were also obtained for the SO_2-oxidized catalysts after reduction at 250 °C in H_2. The fits are given in Table 6. The XANES spectra were similar to those for reduced Pt (see Fig. 9a). Although a portion of the Pt–Pt EXAFS contribution overlaps with the Pt–S contribution (Fig. 9b), the fits clearly indicate that the reduced catalysts contain Pt–S and Pt–Pt bonds. In addition, there are no Pt–O bonds after reduction. Within the limits of accuracy, the size of the reduced particle is unchanged after SO_2 poisoning (e.g., compare Tables 3 and 6). Consistent with the larger metal particle size in the reduced catalysts, the Pt–Pt bond distance increases to about 2.75 Å. As observed for the H_2S-poisoned catalysts, it was not possible to detect Pt–S on Pt(0.10)/silica, and the Pt–S CN increases with decreasing particle size. The presence of Pt–S in the reduced Pt/silica catalysts suggests that SO_2 is bonded to Pt atoms in the oxidized catalysts, since silica does not form surface sulfates as observed on alumina. In addition, since there were no Pt–S contributions to the EXAFS in the SO_2-oxidized sample, the SO_2 was bonded through an oxygen atom, that is, a Pt–O–S–O bond or similar species.

For Pt(0.63)/silica, the structure of Pt is very similar after one or four reactions (and reductions) with SO_2, which is consistent with the catalytic and IR results, indicating that the Pt is rapidly poisoned. For Pt(0.68)/alumina, however, after one catalyst test, the amount of Pt–S is significantly lower than what is found after four reactions. As with the IR and catalytic tests, EXAFS indicates that at short TOS, the Pt/alumina is less poisoned by SO_2 than is Pt/silica.

4. Discussion

The results presented in this paper show that the effect of sulfur on Pt catalysts during CO oxidation is a dynamic phenomenon that strongly depends on the catalyst's history, including (1) how sulfur is added, (2) the pretreatment used before reaction, (3) the type of support used, (4) crystallite size, (5) the reaction conditions, and (6) the TOS at which measurements are made. The results show how critical is the use of operando techniques to correlate the state of the surface with the catalytic activity.

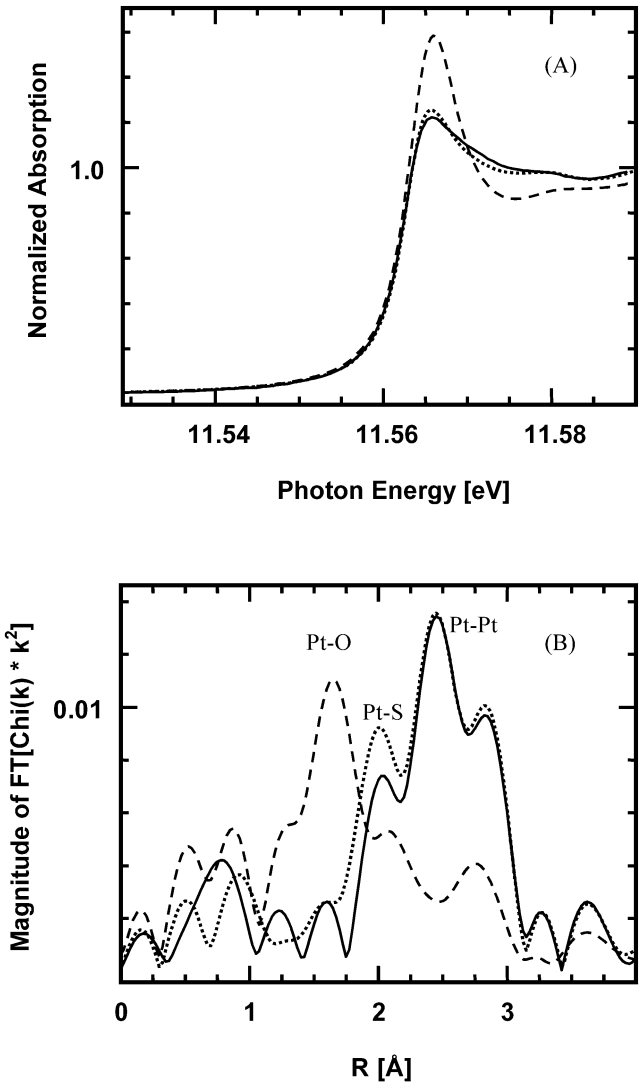

Fig. 9. (A) Normalized XANES spectra for the 2% Pt(0.63)/silica catalyst from 11.53 to 11.59 keV, oxidized by SO_2 and reduced (reduced, solid lines; oxidized by SO_2, dashed lines). (B) Magnitude of the k^2-weighted FT ($k = 2.75$–13.2 Å^{-1}) for 2% Pt(0.63)/SiO_2, oxidized by SO_2 and reduced (reduced, solid lines; oxidized by SO_2, dashed lines).

Ex situ S poisoning is often used because it is a simple way to dose S on the catalyst surface without contaminating the reaction apparatus. Conversion results after ex situ S poisoning, however, might be misleading because the reaction mixture or the pretreatment can remove some of the initially loaded S, and those results would correspond to a surface in a transient state. Under such conditions, it is difficult to correlate the conversion with the initial amount of sulfur loaded, which depends on the catalyst's history before the activity measurements. The type of reactor used can also affect the results, as was the case in the recycle reactor versus the results in the ten-channel parallel reactor. Because of the large internal recycle flow (about 20 times higher than the flow in a single channel) in the recycle reactor, the reactants removed the initial sulfur rapidly after an exponential decaying residence time distribution typical of a well-mixed flow. The sulfur thus removed was trapped in the recycle loop, and therefore its effect on the activity was not observed. In the ten-channel parallel reactor, however, the flow pattern is plug flow and is an order of magnitude smaller than in the recycle reactor. In this case the fraction of sulfur removed by the reacting gases was carried down the bed and re-adsorbed by the support on the Pt surface. Thus S was transported in a slow-moving wave that did not break through from the beds during the TOS used in these experiments. Thus the experiments in the parallel reactor showed the effect of the initial H_2S poisoning in the LOT, whereas this was not observed in the recycle reactor.

During the co-feed experiments, a quasisteady-state equilibrium concentration is achieved on the Pt surface because as S is removed by the reactants, it is replaced by the S supplied by SO_2 in the gas phase. Hence co-feeding experiments are representative of quasisteady-state conditions independent of the reactor used, and thus only co-fed experiments conducted thereafter are discussed below. In such experiments the results depended on the pretreatment used and TOS, as well as the catalyst dispersion and type of support used. The discussion below shows that many of these effects are a consequence of sampling the surface under different TOS, reflecting different surface conditions.

The activity and repeated IR experiments show that apparently Pt/SiO_2 is more susceptible to S poisoning than Pt/Al_2O_3. This apparent support effect is explained by the sulfur storage capacity of alumina, which retains sulfur on its surface, forming sulfates and thus delaying the poisoning of the Pt surface. Eventually, after the alumina surface is saturated by sulfur, alumina- and silica-supported catalysts have the same LOT, that is, the same activity. These observations agree with studies showing that sulfur compounds (H_2S and SO_2) can form adsorbed sulfate ions on γ-Al_2O_3 or aluminum sulfate in the presence of O_2 and at temperatures greater than 400 °C [30–32]. Although such results were obtained on aluminas without Pt, it is expected that they will also occur to a similar extent in the case of Pt/Al_2O_3. This is actually demonstrated by the IR results in Fig. 7, showing the growth of the sulfate bands with TOS. Chang [31] suggested that on Pt/Al_2O_3 the formation of surface sulfates occurs via spillover of oxidized SO_3 onto the Al_2O_3 surface. On the other hand, the SiO_2 support, which is less reactive to the formation of surface sulfates, shows no IR bands for sulfate species, showing that no S storage occurs on the support. Thus, on silica, S poisoning affects the Pt surface without the delay observed in the case of alumina. Gandhi and Shelef [33] reported that in studies of SO_2 oxidation over automotive catalysts, the SO_3 formed is chemisorbed on the γ-Al_2O_3 surface in the form of aluminum sulfate. At elevated temperatures the stored sulfur is emitted as a mixture of SO_2 and SO_3, depending on the temperature and oxygen pressure.

The IR results at short TOS (Figs. 5–7) show little effect of S on the IA of adsorbed L-CO, and that no bridge-bonded

Table 6
EXAFS results for 2% catalysts poisoned by SO_2 and reduced at 250 °C

Composition	Dispersion (%)	Scattering atoms	CN (±10%)	R (Å) (±0.02)	Δ DWF ($\times 10^3$ Å^2)	E_0 (eV)
SiO_2	0.10	Pt–Pt	11.3	2.77	1.6	−1.9
SiO_2	0.33	Pt–Pt	9.0	2.76	1.6	−2.5
		Pt–S	0.5	2.30	4.0	2.2
SiO_2	0.63	Pt–Pt	7.5	2.75	1.6	−2.7
		Pt–S	0.7	2.30	4.0	1.7
SiO_2 (4X SO_2)	0.63	Pt–Pt	8.5	2.76	1.6	−3.1
		Pt–S	0.6	2.30	4.0	2.0
5%CeO_2–SiO_2 (No SO_2)	0.72	Pt–Pt	7.6	2.74	1.6	−3.0
5%CeO_2–SiO_2	0.72	Pt–Pt	7.2	2.75	1.6	−2.7
		Pt–S	0.3	2.30	4.0	2.0
Al_2O_3	0.68	Pt–Pt	5.5	2.74	1.6	−4.1
		Pt–S	0.3	2.30	4.0	0.9
Al_2O_3 (4X SO_2)	0.68	Pt–Pt	5.1	2.74	1.6	−4.4
		Pt–S	1.3	2.30	4.0	2.7
5%CeO_2–Al_2O_3 (No SO_2)	0.73	Pt–Pt	7.4	2.75	1.6	−2.9
5%CeO_2–Al_2O_3	0.73	Pt–Pt	6.9	2.75	1.6	−3.3
		Pt–S	0.4	2.30	4.0	1.8

CO is detectable. At first, this appeared to be contradictory, since adsorbed S species, not detectable in the middle IR range, were expected to occupy sites that otherwise would be available to CO, thus decreasing CO coverage, as reported by Apesteguia et al. [12]. Our experiments were conducted under operando conditions, and thus the presence of O_2 in the feed affected the results. This is not observed for Pt/SiO_2 or Pt/Al_2O_3, even though there is an increase in the LOT, indicating a decrease in activity. There is, however, a significant change in the frequency of adsorbed CO in consecutive runs from about 2071 cm^{-1} to about 2087 cm^{-1}. Such a large decrease in frequency cannot be due to dipole–dipole interactions, but rather to the weakening of the Pt–CO bond strength. Such a decrease in bond strength should translate into less CO inhibition and thus into a *lower* LOT instead of the higher values observed. The shift in frequency can be rationalized because the interaction of electron acceptors such as adsorbed sulfur species would decrease the back-donation of the electrons from Pt to CO, thus weakening the CO–Pt bond. Similar IR results by Bartholomew et al. [1] show that at low coverage, S has little effect on the intensity of the L-CO band and that no bridge-bonded CO was observed. Such experiments at low sulfur coverage are equivalent to experiments at low TOS, as reported in this work. A study comparing the competitive adsorption of SO_2 and CO on supported noble metal catalysts by Gandhi [34] shows that supported Pt co-adsorbed both gases, which agrees with the explanation of the frequency shifts observed in the IR results.

The accelerated aging experiment (Fig. 8) is interesting in several aspects. It shows that once Pt is exposed to SO_2 for a long TOS in the absence of reaction, there is little CO absorption at room temperature. Once the reaction mixture enters the IR cell in operando mode and the temperature increases, the reactants themselves are capable of removing some of the S, but not all, until a quasiequilibrium condition is reached, and there is sufficient CO adsorbed to ignite the catalysts. The frequency of the L-CO band observed in these experiments is equal to the maximum value observed in the short TOS experiments and does not change with temperature. Pre-reduction (in H_2) of the SO_2-treated surface for 3 h at 200 °C is not able to remove the sulfur, indicating that some critical coverage has been reached of irreversible adsorbed sulfur that cannot be reduced by hydrogen but part of which can be removed by the reactants. The LOT observed after the accelerated aging runs is the highest observed in the IR studies. No such long-term experiments were conducted in the presence of the reaction mixture, but we speculate that it will take a very long TOS run to reach the S coverage obtained in the accelerated poisoning experiments.

It remains to explain why the activity decreases (higher LOT) if CO coverage is only slightly altered and the CO bond is actually weakened by SO_2. The explanation must reside on the other undetected adsorbate in the mid-IR range, namely oxygen, whose dissociation must be altered by sulfur. In fact, as pointed out in the Introduction, Bonzel and Ku [10] showed that on Pt(100), adsorbed sulfur considerably weakens the CO-metal bond and that the rate of CO_2 formation on Pt(100) is completely inhibited at sulfur coverages equal to or greater than 0.3, even though CO can still be adsorbed. The decrease in reaction rate was explained by the inhibition of O_2 dissociation on the Pt surface. Ruckenstein et al. [9] reached the same conclusion based on theoretical studies. A similar result was obtained during S adsorption on Pt and Ni single crystals [6], and it was postulated that the effect of S on these metals is primarily electronic, reducing the availability of metal d-electrons and weakening the interaction with adsorbates. In our case, we can speculate that

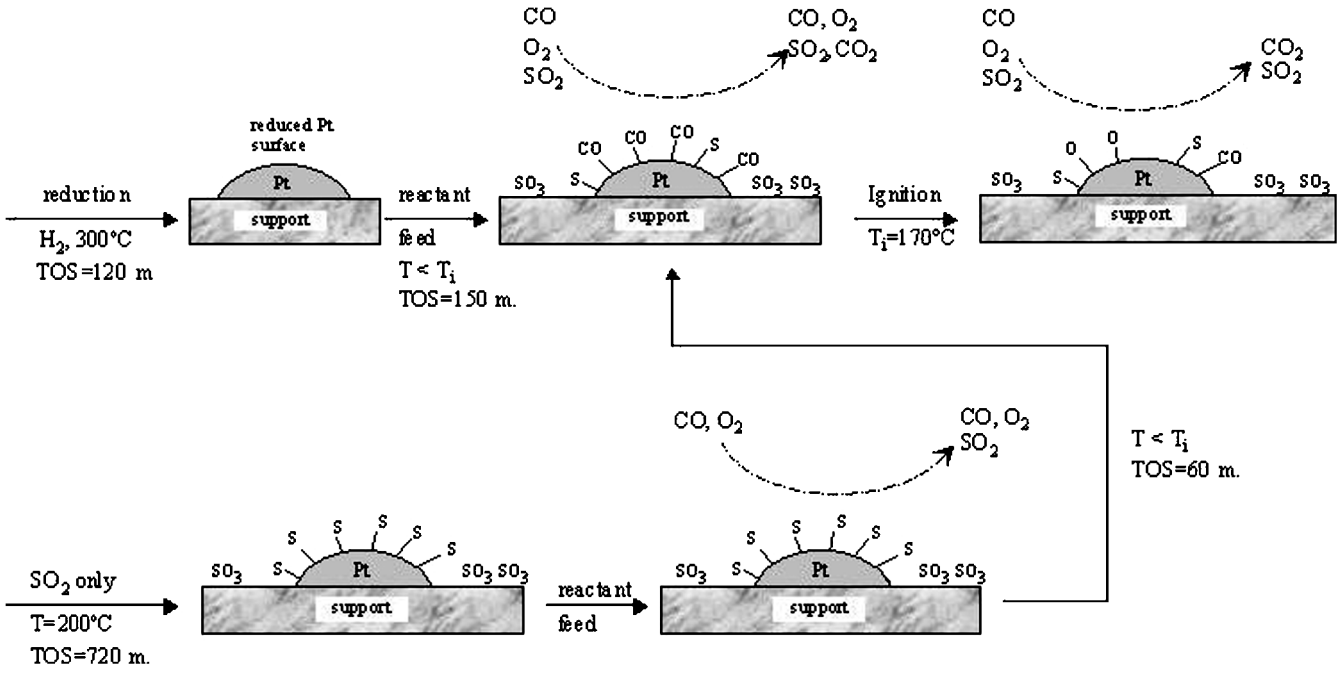

Fig. 10. Cartoon of the poisoning pathway depending on initial conditions and various treatments used for the Pt surface during CO oxidation and in the presence of SO_2 in the feed.

the S coverage was little affected by the hydrogen reduction before each experiment, and it did not reach a level sufficiently high to affect CO adsorption. It is clear, however, that it was sufficient to inhibit O_2 adsorption and dissociation, thus increasing the ignition temperature. The disappearance of the bridge-bonded CO band indicates that those sites were covered by S, suggesting that such sites are relevant to the initiation of oxygen dissociation and were responsible for the increase in the ignition temperature as the S coverage of such sites increased. From the EXAFS analysis, the surface Pt forms a Pt–S bond and is Pt^{2+} rather than metallic. O_2 likely requires metallic Pt to be dissociated. In addition, S is thought to be coordinated in threefold hollow sites on Pt. Since O_2 will require more than one Pt atom to dissociate, upon S poisoning there appear to be few regions of the surface where several S-free, metallic Pt atoms are present.

Another point that is evident from the activity results shown in Table 4 is that the TOF depends on crystallite size. This is first seen in the results obtained without SO_2, in which the TOF of the catalyst with a low dispersion ($d = 0.33$) has a higher TOF than the highly dispersed catalysts ($d = 0.63$). Similar results were reported recently in a previous study on unpoisoned catalysts [22]. Upon the addition of SO_2, the TOF decreases in all Pt/SiO_2 catalysts but remains the highest in the catalysts with $d = 0.33$. The catalysts with the lowest dispersion ($d = 0.1$) show the lowest activity because in this case the low active area yields a lower activity over the increase obtained in the intermediate-size crystallites versus the highly dispersed ones. We interpreted these crystallite size effects on unpoisoned catalysts via dynamic Monte Carlo simulations. The simulations agreed with experimental results only when the smallest crystallites had corner and edge sites with 10 times lower activity than sites located on terraces. The lower activity could arise from a stronger CO–Pt bond in these low coordination sites, which in turn are less active toward CO oxidation. A similar argument can be invoked in the presence of S, which should adsorb on the sites of lower coordination, that is, corner and edge sites. This will make the crystallite size effect even more pronounced, as seen in the TOF at 150 °C. This would be particularly important if such sites are also involved in oxygen dissociation. In the absence of S the difference in rate in catalysts with different dispersion is only a factor of about 2 larger on the catalysts with intermediate and highest dispersion. In the presence of S, however, the difference in the TOF is a factor of about 5 with and without S.

The EXAFS results were obtained in situ but not under operando conditions and thus can indicate only the initial state of the surface. The most important result obtained from these experiments is that no Pt–S signal fit the results in the SO_2-poisoned catalysts. This suggests that in this case S is bonded to O species adsorbed to Pt, which agrees well with the conclusion that S is inhibiting oxygen-dissociative adsorption instead of CO adsorption.

Based on the activity, operando IR, and in situ EXAFS studies, we proposed the model presented in Fig. 10 to explain the results obtained during the ex situ H_2S and SO_2 co-feeding experiments. The relative surface coverages of CO, adsorbed S species, and adsorbed oxygen are affected by the temperature, the gas composition, and TOS. The later variable determines the approach to quasisteady-state conditions. The activity and IR results showed that when 20 ppm of SO_2 are added to the gas phase, the ignition temperature of Pt catalysts supported on silica and alumina during CO

oxidation increases by at least 20 °C. It can then be expected that this poisoning effect would be greater with higher SO_2 concentrations. Indeed, in a study of the effect of sulfur on commercially produced Pd and Pt–Rh automotive catalysts [35], Beck and Sommers showed that increasing the sulfur concentration from 0 ppm to 10, 20, or 30 ppm of SO_2 in the reactant mixture resulted in a LOT increase during CO oxidation of 35, 40, and 50 °C, respectively. Our IR results indicate that, under reaction conditions and with increasing catalyst temperature, a quasisteady-state coverage of CO, adsorbed S species, and O_2 is established on the Pt surface, and the catalysts reaches ignition at a temperature higher than in the case of a SO_2-free reactant feed. After ignition most of the CO is quickly converted to CO_2. On the other hand, after a 12-h poisoning treatment with SO_2 *in the absence* of CO or O_2 in the gas phase, the Pt surface is covered by sulfur, and little CO chemisorption is observed right after resumption of the reactant's flow. As the temperature is increased, CO removes part of the sulfur from the Pt surface and CO adsorption reaches levels similar to those previously observed on the equilibrated catalysts.

The results presented in this paper clearly demonstrate that the state of the surface is a dynamic process depending on the kinetics of surface transformation, temperature, reactant concentration, TOS, and even the reactor used, all of which determine the structure and composition of the Pt surface. In short TOS experiments, in which the surface is not equilibrated, the conditions can be different from those in long-term experiments, where the surface reaches a quasiequilibrium state. Comparison of results from different research groups requires detailed examination of all the conditions used to draw valid conclusions. Although this is a common sense conclusion, researchers often compare results obtained under quite different conditions, such as single crystal versus supported catalysts, to cite a common example. Often heated arguments about which interpretation is the correct one are just a reflection of the fact that the surfaces are being observed under different states because of the use of different experimental parameters.

5. Conclusions

The results presented in this work show that sulfur poisoning of supported Pt catalysts during CO oxidation not only affects the bonding of adsorbed CO molecules on the Pt surface, but also occurs by blockage of the active sites where oxygen adsorbs dissociatively, increasing the ignition temperature. The initial extent of the poisoning is determined by the storage capacity of the support, which prevents the poison from adsorbing to the active sites. After this capacity has been exhausted with time on stream in the presence of SO_2, the activity and in situ IR results indicate no effect of the support on the catalyst's activity.

The results obtained during ex situ treatment with H_2S and when SO_2 is co-fed in the reactant mixture suggest that the pretreatment and the reaction conditions affect the state of the surface and the equilibrium surface coverages. A reduction pretreatment removes part of the sulfur blocking the Pt surface after ex situ H_2S pretreatment, allowing CO to adsorb. The remaining adsorbed sulfur is oxidized under reaction conditions and can be completely removed by the reactants. When SO_2 is continuously added to the reaction mixture, both CO and SO_2 are adsorbed on the Pt surface. The equilibrium surface coverages that determine the overall activity are determined by the relative concentrations in the gas phase and the reaction temperature. A model is proposed to explain the experimental results obtained in this work.

Acknowledgments

Use of the Advanced Photon Source was supported by the US Department of Energy, Office of Basic Energy Sciences, Office of Science (DOE-BES-SC), under Contract no. W-31-109-Eng-38. The MR-CAT is funded by the member institutions and DOE-BES-SC under contracts DE-FG02-94ER45525 and DE-FG02-96ER45589. We also acknowledge funding of this work from a National Science Foundation grant (NSF 01 38070).

References

[1] C.H. Bartholomew, P.K. Agrawal, J.K. Katzer, Adv. Catal. 31 (1981) 135.
[2] J. Oudar, H. Wise, Deactivation and Poisoning of Catalysts, Dekker, New York, 1985.
[3] G.A. Somorjai, J. Catal. 27 (3) (1972) 453.
[4] L.D. Schmidt, D. Luss, J. Catal. 22 (1971) 269.
[5] P.J.F. Harris, Nature 323 (1986) 792.
[6] J. Oudar, Mater. Sci. Eng. 42 (1980) 101.
[7] V.O. Thomas, J.W. Schwank, J.L. Gland, Surf. Sci. 464 (2000) 153.
[8] M. Kiskinova, A. Szabo, J.T. Yates Jr., J. Chem. Phys. 89 (12) (1988) 7599.
[9] L. Halachev, E. Ruckenstein, J. Catal. 73 (1982) 171.
[10] H.P. Bonzel, R. Ku, J. Chem. Phys. 58 (1973) 4617.
[11] P.J. Feibelman, D.R. Hamann, Phys. Rev. Lett. 52 (1) (1984) 61.
[12] C.R. Apesteguia, C.E. Brema, T.F. Garetto, A. Borgna, J.M. Parera, J. Catal. 89 (1984) 52.
[13] K. Wilson, C. Hardacre, R.M. Lambert, J. Phys. Chem. 99 (38) (1995) 13755.
[14] K. Wilson, C. Hardacre, R.M. Lambert, Div. Pet. Chem. Am. Chem. Soc. 41 (1) (1996) 37.
[15] K. Wilson, R.M. Lambert, C. Hardacre, SO_2-Promoted Propane Oxidation Over Pt(111) and Pt(111)/AlO_x Model Systems, Programme–11th mt. Congr. Catal.–40th Anniv. (June 30–July 5, 1996), Po-278.
[16] A.F. Lee, K. Wilson, R.M. Lambert, C.P. Hubbard, R.G. Hurley, R.W. McCabe, H.S. Gandhi, J. Catal. 184 (1999) 491.
[17] G.P. Ansell, S.E. Golunski, H.A. Hatcher, R.R. Rajaram, Catal. Lett. 11 (1991) 183.
[18] V. Meeyoo, D.L. Trimm, N.W. Cant, Appl. Catal. B 16 (1998) L101.
[19] Yi. Wang, PhD Dissertation, New Jersey Institute of Technology, 1995.
[20] R. Burch, P. Fornaserio, B.W.L. Southward, Chem. Comm. 625 (1998).
[21] J.T. Miller, M. Schier, A.J. Kropf, J.R. Regalbuto, J. Catal. 225 (2004) 203.

[22] F.J. Gracia, L. Bollman, E.E. Wolf, J.T. Miller, A. Kropf, J. Catal. 220 (2003) 282.
[23] W. Li, F.J. Gracia, E.E. Wolf, Catal. Today 83 (2003) 437.
[24] C.U. Segre, N.E. Leyarovska, W.M. Lavender, P.W. Plag, A.S. King, A.J. Kropf, B.A. Bunker, K.M. Kemmer, P. Dutta, R.S. Duran, J. Kaduk, in: P. Pianetta, et al. (Eds.), CP521, Synchroton Radiation Instrumentation: 11th US National Conference, American Institute of Physics, New York, 2000, p. 419.
[25] T.J. Ressler, J. Sync. Rad. 5 (1998) 118.
[26] F.W. Lytle, D.E. Sayers, E.A. Stern, Physica B 158 (1989) 701.
[27] M. Shelef, G. Graham, Catal. Rev. Sci. Eng. 36 (1994) 433.
[28] D.O. Simone, T. Kennelly, Appl. Catal. 70 (1991) 87.
[29] A.J. Frenkel, C.W. Hills, R.G. Nuzzo, J. Phys. Chem. B 105 (51) (2001) 12689.
[30] A.V. Deo, I.G. Dalla Lana, H.W. Habgood, J. Catal. 21 (1971) 270.
[31] C.C. Chang, J. Catal. 53 (3) (1978) 374.
[32] Y. Okamoto, M. Oh-Hara, A. Maezawa, T. Imanaka, S. Teranishi, J. Phys. Chem. 90 (1986) 2396.
[33] H.S. Gandhi, M. Shelef, Appl. Catal. 77 (1991) 175.
[34] H.S. Gandhi, H.C. Yao, H.K. Stepien, M. Shelef, SAE paper 780606 (1978), in special publication SP-431.
[35] D.D. Beck, J.W. Sommers, in: A. Frennet, J.M. Bastins (Eds.), Catalysis and Automotive Pollution Control III, Studies in Surface Science and Catalysis, vol. 96.